PERGAMON

Vacuum 58 (2000) 263–271

VACUUM
SURFACE ENGINEERING, SURFACE INSTRUMENTATION & VACUUM TECHNOLOGY

www.elsevier.nl/locate/vacuum

# An investigation of a Cd–Ne afterglow plasma☆

Ts. Petrova[a], A. Ogoyski[b], G.M. Petrov[c], A. Blagoev[a,*]

[a]*Faculty of Physics, Sofia University, 5 James Bourchier Boulevard, BG-1164 Sofia, Bulgaria*
[b]*Department of Physics, Technical University, 2 Studentska Str., BG-9001 Varna, Bulgaria*
[c]*Institute of Solid State Physics, Bulgarian Academy of Sciences, 72 Tzarigradsko Chaussee Boulevard, BG-1784 Sofia, Bulgaria*

**Abstract**

An investigation in the afterglow of a Cd–Ne positive column at low and intermediate pressure is presented. The model is based on numerical solution of the time-dependent Boltzmann equation and a system of particle balance equations for the electrons, excited atoms and ions. By this model all discharge properties of interest (electron energy distribution function, electron and ion densities and the populations of both Cd and Ne excited states) are calculated in the afterglow. The populations of the excited Cd ($5p^3P_{0,1,2}$) atoms are measured using time-resolved optical absorption spectroscopy. The electron density is derived by probes measurements. Model predictions are in fair agreement with measured electron density and excited-state populations. 

*Keywords:* Cd vapour; Plasma afterglow; Modelling; Boltzmann equation; Optical absorption; Probes

## 1. Introduction

Noble gas–metal vapor discharges have been widely investigated and their properties well known. They are used for lasers (He–Cd, He–Zn, He–Hg, etc.), hollow cathode lamps and spectroscopic and light sources. Usually, the metal ion is involved and except Hg, most of these investigations refer to the ion, rather than to the atom. Investigations of the metal atom are lagging behind despite their unique applications. For example, for more than 30 years, Hg is used as a light source and it would be natural to assume that other metals may have similar application.

☆Paper presented at the 11th International School on Vacuum Electron and Ion Technologies, 20–25 September 1999, Varna, Bulgaria.

* Corresponding author. Tel.: + 359-2-62-56-344; fax: + 359-2-96-25-276.
*E-mail address:* blagoev@phys.uni-sofia.bg (A. Blagoev).

0042-207X/00/$ - see front matter 
PII: S0042-207X(00)00177-9

Mercury-free discharge as a light source is a hot topic and the leading laboratories are currently searching for discharges, capable of emitting efficient visible or UV radiation. Investigations in the late 1960s revealed that Cd could be more efficient compared to Hg as a light source [1]. The steady-state model we have recently developed suggests that Cd indeed has higher efficiency compared to Hg of converting the input power into UV radiation, reaching the impressive value of 80% at idealized discharge conditions [2]. This and other prospective applications prompted us to further investigate this discharge. Our objectives are to investigate theoretically and experimentally the discharge properties of a Cd–Ne positive column and in particular the electron density, the resonance states $5p^3P_1$ and $5p^1P_1$ and the metastable states $5p^3P_0$ and $5p^3P_2$ in the afterglow.

## 2. Basic relations

### 2.1. Collisional-radiative model

It is well known that the main properties of the electron and heavy-particle kinetics are determined by the metal and the noble gas in most of the cases is only a buffer gas limiting the charged particle and metastable states diffusion. Hence, a comprehensive model for Cd atom is crucial for accurate determination of the discharge properties. Recently, we have compiled a set of data (cross sections and rate coefficients) for Cd and a steady-state model was developed, which is the backbone of the present model. The Cd models used in this and our former work could be summarized as follows.

Five Cd excited states are considered in the study: the resonance $5p^3P_1$ and $5p^1P_1$ states, one effective metastable $5p^3P_{2,0}$ state ($5p^3P_0$ and $5p^3P_2$ metastable states are treated as one effective block of levels), $6s^3S_1$ and one $5d^3D_{1,2,3}$ lumped block of levels (Fig. 1). The only considered ion is the Cd atomic ion ($Cd^+$); the molecular ion plays a minor role. For these excited states/blocks of levels the following processes are considered: direct and stepwise excitation and deexcitation by electrons, ionization, spontaneous emission to lower lying states (including trapping of the resonant radiation), diffusion of the metastable to the wall, transitions between the effective

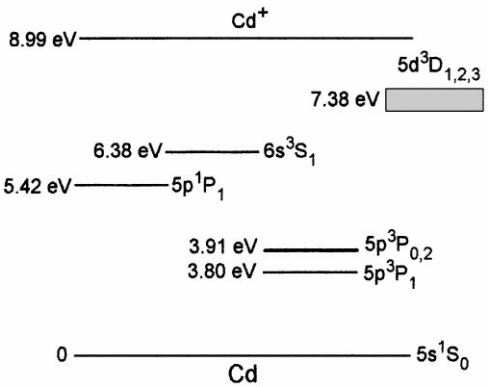


Fig. 1. An energy level diagram of Cd atom.

metastable state and the resonance state in the triplet and energy pooling collisions between the two $5p^3P_1$ excited atoms. It is assumed that the main loss channel for $Cd^+$ is diffusion to the wall. The role of Ne in the model is limited, considering only diffusion of Cd ions and metastable states in Ne.

### 2.2. Balance equations

For each excited state and charged particle the balance equation must be solved. Unlike our former model [2], the present model considers the afterglow and the balance equations are time dependent. Written in a short form, convenient for numerical calculations, each balance equation reads

$$\frac{dN_k(t)}{dt} = S_k(t), \tag{1}$$

where $S_k(t)$ comprises all creation and loss terms. These terms generally depend on the populations of the excited states and charged particle densities as well as the rate coefficient for each particular reaction. The rate coefficients involving electrons require the knowledge of the electron energy distribution function (EEDF) at any moment in the afterglow.

### 2.3. Electron energy distribution function

An investigation of the temporal relaxation of the electrons in the afterglow is performed by solving time-dependent electron Boltzmann equation for spatially homogeneous plasma using the conventional two-term Legendre polynomial expansion of the electron velocity distribution function (EVDF). The electron Boltzmann equation includes collision processes such as elastic collisions (electron–electron, electron–ion and electron–atom), inelastic collisions (excitation and ionization) and ambipolar diffusion described by generalized diffusion frequency $\nu^{\mathrm{diff}} = (\mu/R)^2 D_a$, where $D_a$ is the ambipolar diffusion coefficient and $\mu = 2.405$ for Bessel profile of the charged particles.

Following the above-mentioned assumption, the electron Boltzmann equation for the isotropic part of the EVDF $f_0$ can be written in form

$$\begin{aligned}
&\frac{u^{1/2}}{v_0}\frac{\partial f_0(t,u)}{\partial t} + \frac{\partial}{\partial u}\left\{\frac{2}{3}\Gamma^{ee} g(t,u)\frac{\partial f_0(t,u)}{\partial u} + \left[\sum_{\alpha=\mathrm{Ne},\ \mathrm{Cd}} \frac{2m}{M_\alpha} u^2 N_\alpha Q_\alpha^{el}(u) + \Gamma^{ee} h(t,u)\right] f_0(t,u)\right\} \\
&\quad - \sum_i N_i u Q_i^{in}(u) f_0(t,u) - \frac{\nu^{\mathrm{diff}}}{v_0} u^{1/2} f_0(t,u) \\
&= -4\sum_i N_i (2u + U_i^{ion}) Q_i^{ion}(2u + U_i^{ion}) f_0(t, 2u + U_i^{ion}) \\
&\quad - \sum_i N_i (u + U_i^{exc}) Q_i^{exc}(u + U_i^{exc}) f_0(t, u + U_i^{deexc}) \\
&\quad - \sum_i N_i (u - U_i^{deexc}) Q_i^{exc}(u - U_i^{deexc}) f_0(t, u - U_i^{deexc}),
\end{aligned} \tag{2}$$

where $t$ is the time, $u$ the electron energy (in eV), $n_e$ the electron density, $2m/M$ the electron to atom mass ratio, and $v_0$ the velocity of the electron with kinetic energy of 1 eV. $M$, $N$, and $Q_\alpha^{el}(u)$ are the mass, density and the momentum transfer cross section of the neutral particles (Cd and Ne atoms). $Q_i^{in}(u)$ stands for excitation, deexcitation or ionization cross section and $\Gamma^{ee} = (e^2/24\pi\varepsilon_0^2)\ln\Lambda$, where $\ln\Lambda$ is the Coulomb logarithm. The right-hand side accounts for the in- and out-scattering terms of electrons by excitation, deexcitation and ionization. The $i$th excitation process is characterized by excitation cross section $Q_i^{exc}$, energy threshold $u_i^{exc}$ and density $N_i$ of the initial state. The deexcitation and ionization processes are defined analogously. The normalization of the EEDF is $\int_0^\infty f_0(t,u)u^{1/2}\,du = n_e(t)$. The effect of the electron–electron collisions is accounted for by inclusion of a Fokker–Planck term, yielding the two integral terms containing $g(t,u)$ and $h,(t,u)$,

$$g(t,u) = \int_0^u u'^{3/2} f_0(t,u')\mathrm{d}u' + u^{3/2}\int_u^\infty f_0(t,u')\mathrm{d}u', \quad h(t,u) = \int_u^\infty u'^{1/2} f_0(t,u')\mathrm{d}u'$$

in Eq. (2)

After an appropriate energy space averaging of the electron Boltzmann equation the consistent electron particle balance

$$\frac{\mathrm{d}}{\mathrm{d}t} n_e(t) = \sum_i \Gamma_i^{ion}(t) - \nu^{diff} n_e(t) \tag{3}$$

and the electron energy balance

$$\frac{\mathrm{d}}{\mathrm{d}t} \bar{u}(t) = P^{deexc}(t) - P^{el}(t) - P^{ei}(t) - P^{in}(t) - P^{diff}(t) \tag{4}$$

are obtained. $\Gamma_i^{ion}$ is the rate of the $i$th ionization process, $\bar{u}(t) = \int_0^\infty u^{3/2} f_0(t,u)\mathrm{d}u$ is the mean electron energy density and $P$ denotes the corresponding electron energy gain or loss. $P^{deexc}(t)$ is the energy gain for the electrons due to deexcitation, $P^{el}(t)$ and $P^{ei}(t)$ are the electron energy loss due to elastic electron–atom and electron–ion collisions, $P^{in}(t)$ is the loss of the energy in inelastic collisions and $P^{diff}(t)$ is the energy loss due to radial diffusion.

The partial differential equation (2) for the EEDF has been solved as an initial-time value problem [3] using a numerical technique based on finite difference approach. At $t = 0$ $f_0(0,u) = f_0(u)$, where $f_0(u)$ is the EEDF, obtained from homogeneous electron Boltzmann equation.

### 2.4. Self-consistent coupling

The time-dependent electron Boltzmann equation is self-consistently coupled with a system of balance equations for all species considered (excited states and ions), whose solution gives the population of all excited states, atomic and molecular ion densities as a function of the time. The time $t = 0$ corresponds to the moment the discharge is switched off. All quantities (EEDF, populations and densities) are calculated using the steady-state model at given discharge current [2], corresponding to the pulse current amplitude. At each time-step $t$, except $t = 0$, the EEDF and

the new densities are calculated using the values from the calculations of the former time position $t - \Delta t$. Though the procedure seems explicit, it is actually iterative, because the EEDF at time $t$ depends on the electron density and the populations of the excited states at the same time step, which in turn depend on the EEDF. Hence, the EEDF and the balance equations must be treated together.

The numerical procedure requires the following input parameters: tube radius, Ne gas pressure, temperature of the Cd vapor or Cd pressure, a set of atomic data for both gases and initial values for both the homogeneous EEDF $f_0(u)$ and the densities of all particles under consideration at time $t = 0$.

## 3. Experiment

A pulse periodic DC discharge was fired in a quartz cell with 1 kHz repetition rate. The cell radius is $r = 1.5$ cm, its optical path length is 24 cm. The required gas temperature $T_g$ was ensured by an oven. The Cd vapor enters the volume from a side arm compartment with a separate heating. The temperatures were monitored with precision of 1 K. The experiments were carried out in the 515–565 K temperature range. The Cd vapor pressure was varied between 0.36 and 4 Pa. Fig. 2 shows schematically the experimental device. The populations of the excited Cd($5p^3P_{0,1,2}$) atoms have been determined using optical absorption measurements with a bell-bloom lamp (BBL) as a light source. It operates in the same mode as the absorption cell in order to ensure similar conditions in the emission and absorption volumes. The spectrometer that selects the chosen spectral line is supplied with a S-20 photomultiplier FEU-106. A PC-based automated system controlled the operation of the whole system. An extensive description of the system modules and routines was given previously [4]. The relative absorption was recorded on the lines of the visible triplet (508.6, 480, and 468.8 nm). The dependence "*absorption vs. opacity*" is calculated by taking into account the isotope and hyperfine structure of the lines.

Two electric probes introduced in the positive column determined the electric fields used in the conductivity measurements of the electron density.

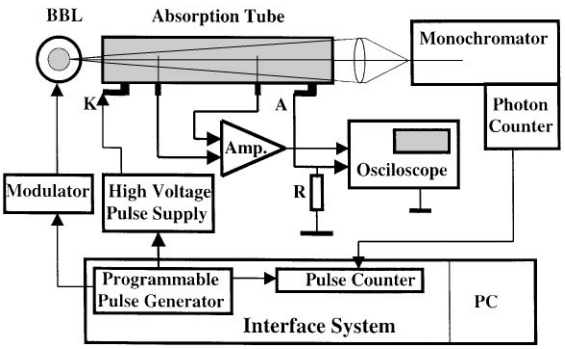


Fig. 2. Experimental setup.

## 4. Results and discussion

In this section, both theoretical and experimental results are presented. We start with example at typical discharge conditions: Ne gas pressure of 66.7 Pa, gas temperature of 551 K (corresponding to 2.31 Pa Cd pressure) and discharge current 20 mA.

The calculated EEDF is shown in Fig. 3. Changes in the distribution function occur as early as 0.1 μs. In the early stage of the decay, the tail of the EEDF is extensively depopulated due to inelastic collisions with Cd atom. The time scale of these processes is typically 1 μs. Since the EEDF in the inelastic energy region is rapidly depopulated with time, the magnitudes of the excitation and ionization rate coefficients decrease correspondingly. The low-energy part of the EEDF experiences minor changes; the elastic collisions have low effectiveness due to the small electron to atom mass ratio. The mean electron energy $\langle u \rangle = 1/n_e(t) \int_0^\infty u^{1/2} f_0(t, u)\, du$ (Fig. 4) decreases by factor two or so. It should be noted that the time-dependent character of the mean energy reflects only changes of the low-energy part of the EEDF and no information about the high-energy part (the inelastic energy region) can be implied. The latter means that there is no correspondence between

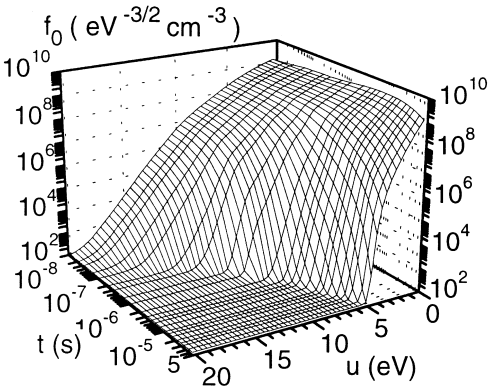


Fig. 3. Calculated EEDF at $p_{Ne} = 66.7$ Pa, $p_{Cd} = 2.31$ Pa, and $i = 20$ mA.

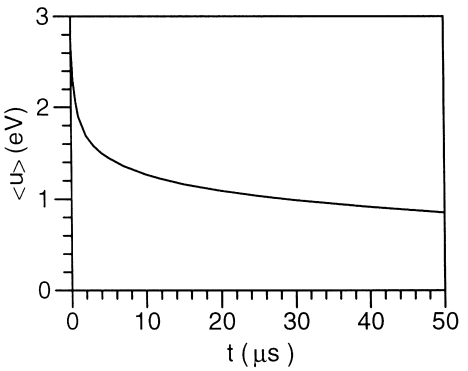


Fig. 4. The mean electron energy at discharge conditions in Fig. 3.

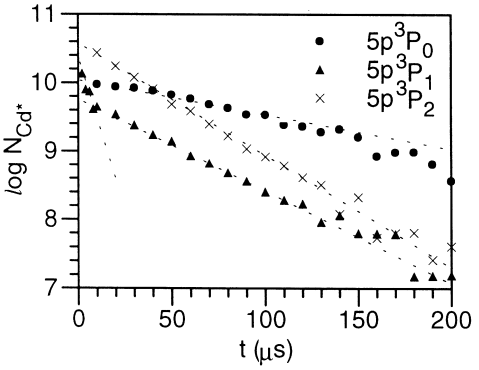


Fig. 5. Measured populations of Cd-excited states at discharge conditions in Fig. 3.

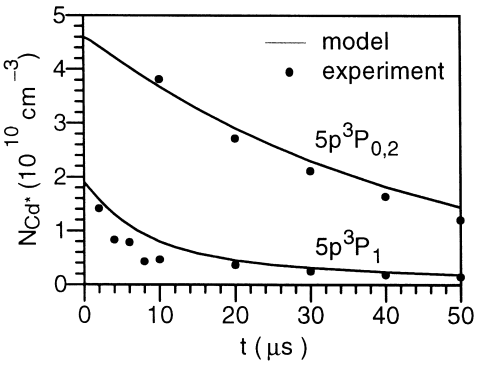


Fig. 6. Measured and calculated populations of Cd-excited states. The discharge conditions are the same as in Fig. 3.

the mean energy $\langle u \rangle$ [or the electron temperature $T_e = (2/3)\langle u \rangle$] and the excitation and ionization rates.

The decay of Cd excited states is shown in Figs. 5 and 6. Fig. 5 displays the experimentally measured decay of both the metastables and the resonance states. The resonance state $^3P_1$ experiences fast initial drop and then follows the populations of the metastables. The fast drop obviously occurs due to radiative decay to the Cd ground state. After time $t > 10$ μs and in the late afterglow the population of the resonance $^3P_1$ state depends on the populations of the metastable states. The $^3P_2$ metastable state has short lifetime, decays very quickly and after 50 μs the dominant excited state is $^3P_0$ state. Fig. 7 shows the calculated and measured densities of the lumped Cd metastable (sum of both metastables) and the resonance state. The model and experiment are in excellent agreement.

One of the most important plasma parameter is the electron density. As mentioned above, the ionization rate becomes negligible only few microseconds after switching off the pulse current and in the electron particle balance equation the creation terms are expected to have small contribution and the electron density decays exponentially with characteristic time determined by the ambipolar diffusion.

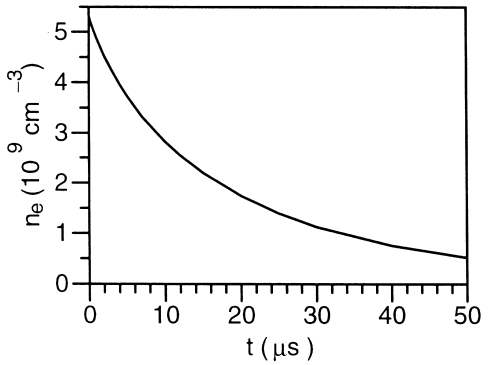


Fig. 7. Calculated electron densities. The discharge conditions are the same as in Fig. 2.

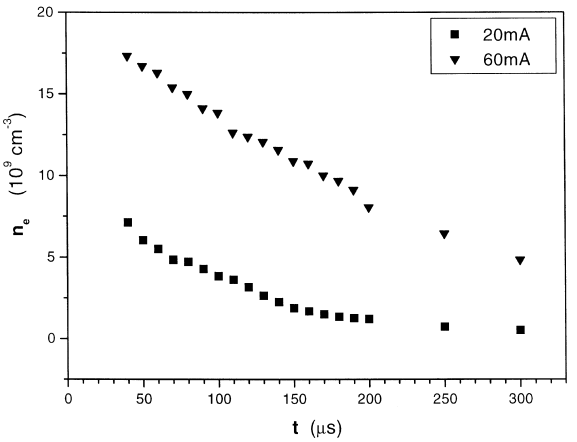


Fig. 8. Decay of the electron density. Discharge conditions: $p_{Ne} = 66.7$ Pa, and $p_{Cd} = 2.31$ Pa.

To give a better overview of the behavior of the electron density in the afterglow, Fig. 8 shows measured electron density at 20 and 60 mA discharge current pulses. The slopes of the decay increases with increase in the discharge current which suggests that the rate of destruction also increases.

## 5. Conclusion

Cd–Ne afterglow discharge has been investigated theoretically and experimentally in the afterglow. The model consists of coupling the time-dependent electron Boltzmann equation to the balance equations for all species considered. The experiment includes both spectroscopic and probes measurements and the decay of several excited states and the electron density has been recorded and analyzed. The comparison of the model and experiment showed that they are in good agreement.

## Acknowledgements

This work was supported by the Bulgarian National Council for Scientific Research under Contract No. F-579/95.

## References

[1] Springer RH, Barnes BT. J Appl Phys 1968;39:3100.
[2] Petrova Ts, Ogoyski A, Petrov GM, Blagoev A. Proc 52 GEC. Bull Am Phys Soc 1999;44:25.
[3] Winkler R, Wuttke MW. Appl Phys B 1992;54:1.
[4] Rusinov IM, Blagoev AB. Bulg J Phys 1996;23:73.